



Engine Oils in the Field: A Comprehensive Tribological Assessment of Engine Oil Degradation in a Passenger Car

Adam Agocs^{1,2} · Charlotte Besser¹ · Josef Brenner¹ · Serhiy Budnyk¹ · Marcella Frauscher¹ · Nicole Dörr¹

Received: 14 October 2021 / Accepted: 18 January 2022 / Published online: 10 February 2022
© The Author(s), under exclusive licence to Springer Science+Business Media, LLC, part of Springer Nature 2022

Abstract

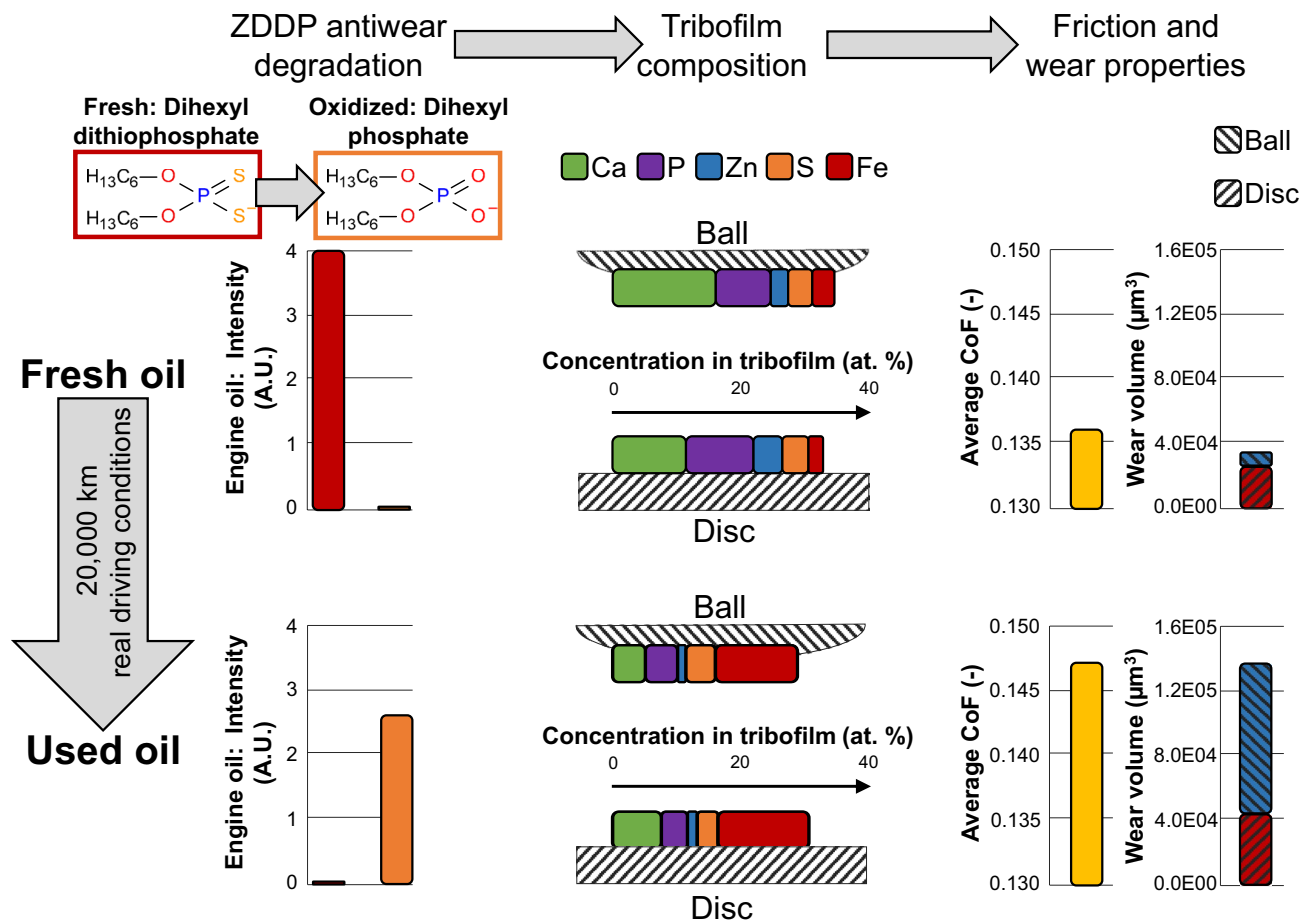
In this study, the deterioration of the friction and wear properties of a SAE 5W-30 engine oil during its service life as well as the differences in tribofilms formed by different oil conditions are investigated. A field test was conducted with a passenger car equipped with a modern, turbocharged gasoline engine under real driving conditions, where several used oil aliquots were collected. The collected used oil samples underwent tribological model tests, which revealed a 9% increase in friction and an over 420% increase in wear compared to the fresh oil during the 20,000 km service life. Furthermore, the composition of the tribofilms was correlated with previously published data on additive degradation in the used engine oils. The observed tribofilms changed significantly depending on additive degradation. In detail, the degradation of zinc dialkyl dithiophosphate (ZDDP) antiwear additive was analysed. The results showed a significant decrease in phosphorus and zinc as well as an increase in iron content in the tribofilms once ZDDP is depleted, which correlates well with the increase in the observed wear rates. Additionally, comparison with high-resolution mass spectrometry data showed that depletion of the original dialkyl dithiophosphate additive and successive formation of dialkyl thiophosphates has only minor influence on the tribofilm composition, the mentioned changes occur once the dialkyl thiophosphates are completely depleted and only dialkyl phosphates remain in the engine oil. This offers some insight on the mechanism of tribofilm formation by in-service, partially degraded ZDDP, which is prevalent under real operating conditions.

✉ Adam Agocs
adam.agocs@ac2t.at

¹ AC2T Research GmbH, Viktor-Kaplan-Straße 2C,
2700 Wiener Neustadt, Austria

² Institute of Chemical Technologies and Analytics, TU Wien
(Vienna University of Technology), Vienna 1060, Austria

Graphical Abstract



Keywords Internal combustion engine oils · Oil condition monitoring · Additive degradation · Antiwear additives · Tribofilm composition · X-ray photoelectron spectroscopy

1 Introduction

According to the European Automobile Manufacturers' Association (ACEA) [1], 94.6% of the new registrations in the European Union (EU) utilized some form of an ICE in the drivetrain in 2020. This shows that internal combustion engines (ICEs) are still the predominant drivetrain technology in automotive and light commercial vehicle applications. Hence, it is safe to assume that ICEs are going to have a considerable market share in the foreseeable future. Consequently, further development of ICEs is an absolute necessity, especially to achieve better emission characteristics and more economical operation.

The interplay of oil condition and tribological performance is fundamental in efficient ICE design [2]. These investigations are especially important, as vehicles with different fuelling are showing significant differences in oil

degradation and oil performance under real driving conditions [3, 4]. Furthermore, the utilization profile also has a significant impact on lubricant performance, as vehicles predominantly used for short trips showed a significantly faster additive depletion and iron accumulation, which is indicative for increased engine wear [3]. Vehicles are predominantly operating on lubricants that are degraded to some degree, as over 20% residual used oil can be expected in a modern passenger car right after the oil change [5]. Accordingly, understanding of the additive degradation and the accumulation of degradation products have a very high technical relevance in component development, resulting in the need to utilize used or artificially altered lubricants in bench testing during ICE (component) development [6–8] to achieve more accurate performance and lifetime predictions.

One of the most well-studied topics regarding oil performance is chemical degradation and performance of

zinc dialkyl dithiophosphate (ZDDP) antiwear additives (AW), as they are commonly used in engine oil applications. Novel, environmentally friendly AW additives are also in the focus of the scientific community since years [9–20]. Accordingly, several studies have investigated the tribological properties of possible ZDDP replacements, such as ashless AW additives [11–13], fluorinated ZDDP (F-ZDDP) [9, 10] as well as ionic liquids [14–20]. The importance of ZDDP on the lubricating properties of engine oils is not diminishing, as highlighted in several reviews [21–23]. The authors also discussed this topic and the corresponding literature in detail in [5].

ZDDP forms a surface layer, commonly referred as tribofilm on metal surfaces, which protects the components from wear. The formation of ZDDP tribofilms is complex, but generally starts at mild temperatures in the wear scar, followed by the growth of the tribofilm [24–29]. Multiple models of the formation as well as the removal of ZDDP tribofilms have been proposed, such as [30–34]. A wide variety of surface-sensitive techniques are used to analyse tribofilms [31–51]. The commonly used analytical methods for tribofilm analysis consist of the following:

- scanning electron microscopy (SEM) and atomic force microscopy (AFM) to analyse the morphology [31, 32, 34, 35, 37–43],
- energy-dispersive X-ray spectroscopy (EDX) and X-ray photoelectron spectroscopy (XPS) to determine the elemental compositions [31–33, 35, 36],
- X-ray absorption near edge structure (XANES) for the analysis of the chemical compositions of tribofilms formed by ZDDP and alternative additives, e.g. [12, 13, 19, 20, 28, 44],
- transmission electron microscopy (TEM) in combination with focussed ion beam sectioning (FIB) for cross-section analysis [45, 46],
- online application of attenuated total reflection infrared spectroscopy (FT-IR ATR) [48, 49],
- X-ray absorbance spectroscopy (XAS) to observe the formation of tribofilms in-situ [50, 51] and
- time-of-flight secondary ion mass spectroscopy (ToF-SIMS) to gain detailed information of the respective masses of the tribofilm-forming compounds [40, 47].

In detail, several articles are reporting on the formation of ZDDP tribofilms. Johnson et al. reports that ZDDP tribofilms are mainly consisting of glassy iron polyphosphate/zinc polyphosphate on top of a thin iron sulphide/zinc sulphide base layer, covered by a zinc polyphosphate layer. The tribofilm is usually deposited in ‘pads’, accordingly, shows an inhomogeneous lateral structure [52]. Gosvami et al. studied ZDDP film growth in model lubricants via in-situ AFM and found that the growth rate of the films increased

exponentially with either compressive stress or temperature, which is consistent with a model involving thermal activation and stress-assistance [43]. Furthermore, they found that iron as catalyst plays only a minor role in the film evolution [43]. Soltanahmadi et al. observed a 5–10 nm thick, separate iron sulphide layer on the substrate via TEM and EDX elemental analysis [45]. Dorgham et al. developed a novel tribometer equipped with synchrotron XAS and showed that shear accelerates the growth of tribo-layers [50]. In a further study they found that the initial surface layer deposits as mainly sulphate, which is later reduced into sulphide under heat and shear [51]. Dawczyk et al. used FIB followed by TEM to study ZDDP tribofilms. They found that FIB changes the morphology of the uppermost 30–50 nm of the tribofilm, but this effect can be counteracted by the deposition of a gold layer prior. They also confirmed a polycrystalline ZDDP-film structure [46]. Sharma et al. investigated the impact of plasma-functionalised polytetrafluoroethylene nanoparticles on the lubrication properties of mineral oils with low levels of ZDDP [53]. They found a dramatic reduction of CoF and overall wear for oils with functionalised nanoparticles. Tribofilm analysis by XPS and XANES clearly proved the presence of Si- and F-doped polyphosphates in tribofilms leading to the suggestion that a protective tribofilm even at reduced ZDDP content is developed by the synergism between plasma-coated nanoparticles and ZDDP. Furthermore, they investigated the effects of ZDDP and titanium dioxide (TiO₂) nanoparticles under a sliding pin-on-disc contact with XPS and XANES [54]. They found that ZDDP and TiO₂ behaved antagonistically with regard of wear protection, although both proved to be a capable antiwear additive on its own.

Most of the mentioned studies are commonly utilizing fresh or model lubricants. Accordingly, the investigation of films formed under real driving conditions, by (partially) degraded ZDDP is largely absent from the literature as used oils are very complex mechanochemical systems, containing a very wide variety of organic structures, which all have a potential influence on the ZDDP tribofilm formation. One exception is the work of Dörr et al., where the authors investigated friction and wear properties and tribofilm formation of a SAE 0 W-20 engine oil after artificial (laboratory) alteration and provided a detailed methodology to assess the influence of lubricant degradation on tribochemistry and the resulting friction and wear properties [55]. In the current study, the methodology described in [55] is used, accordingly, detailed discussion regarding the respective results is presented in 3.3, 3.4 and 3.5. Nevertheless, further investigations seem to be necessary to determine what influence (real) oil degradation has on the ZDDP film growth and composition.

This work aims to bridge the gap between the research regarding ZDDP degradation under real on-road conditions

and tribofilm formation. A field test with a conventional passenger car was conducted under real driving conditions, where used oil aliquots were collected. The authors previously reported the chemical oil condition, such as oxidation, nitration, neutralization number (NN) increase, total base number (TBN) decrease and elemental composition, amongst others, in [5]. The previous work was focussed on ZDDP degradation, where the structure and relative quantity of several degradation products were investigated by advanced mass spectrometry (MS) methods. In this study, tribological evaluation of the collected used oil samples is performed via an Optimol SRV® 5 model tribometer to uncover the deterioration of the friction and wear properties during the service life of an engine oil. Furthermore, XPS is utilized to determine the elemental composition of the tribofilm as well as the chemical state (bonding partners) or the respective elements. XPS is a readily available quantitative measurement technique, which can identify the elemental composition of surfaces. Additionally, information regarding the chemical state of the atoms on the surface can be measured, which allows the deduction of their respective bonding partners.

The XPS results within this study are correlated to the previously published results regarding ZDDP degradation products and oil condition in general, hence, a comprehensive assessment of tribofilm formation and differences in oil condition is achieved.

2 Materials and Methods

The authors previously presented the changes in the chemical composition of an engine oil during a field test conducted with a conventional passenger car in [5]. The study at hand is intended as an extension of the already published

chemical results, focussing on the tribological properties and the chemical composition of the resulting tribofilms of the used engine oil samples obtained from the same field test. Accordingly, the methodology of the performed field test and chemical oil characterization is described in detail in [5] and only a brief summary is presented in 2.1 and 2.2, respectively.

2.1 Field Test

A modern passenger car utilizing a 1.4 L turbocharged petrol engine was surveyed during a typical oil change interval under real driving conditions, mainly consisting of daily commuting, preliminary on a freeway.

A commercially available engine oil with the viscosity class of SAE 5W-30 suitable for both diesel and gasoline engines was applied. The engine oil is blended from a group II or group III base oil with a conventional additive package, containing ZDDP as antiwear additive and calcium carbonate as base reserve. The lubricant has the following original equipment manufacturer approvals:

- ACEA C3,
- API SN,
- BMW longlife-04,
- MB 229.51, MB 229.52,
- VW 502.00/505.00/505.01 and
- GM dexos2™.

Table 1 summarizes the key parameters of both the utilized vehicle according to the certificate of approval as well as the applied lubricant.

At the start of the field test, an oil change was performed 2 times to remove any residual used oil from the engine, ensuring that the obtained oil samples are

Table 1 Key parameters of the applied vehicle and engine oil

Parameters of the vehicle [5]			
Year of manufacture	2013	Mileage at start of test (km)	93,361
Engine configuration	Inline 4 cylinder	Engine aspiration	Turbocharged
Engine displacement (L)	1.4	Power at 4200 min ⁻¹ (kW)	88
Fuel	Gasoline RON 95 (see EN 228 [65])	Fuel injection system	Sequential multi-port fuel injectors
Parameters of the engine oil [5]			
Viscosity at 40 °C (mm ² /s)	65.8	Viscosity at 100 °C (mm ² /s)	11.4
Viscosity index (-)	169	Density at 15 °C (g/cm ³)	0.85
Neutralization number (mg KOH/g)	1.6	Total base number (mg KOH/g)	6.5
Ca content (mg/kg)	1910	P content (mg/kg)	720
S content (mg/kg)	2350	Zn content (mg/kg)	880

representative for the mileage. Subsequently, the vehicle was subjected to a daily commuting routine with a total distance of approx. 110 km a day, of which 75 km (70%) was freeway operation. Used oil aliquots were sampled from the engine in regular intervals. The sampling was performed after a few minutes of idling the engine to ensure oil homogeneity through the dipstick pipe with a suitable PTFE tubing. The engine oil was not refilled during the field test, accordingly, the experiment was terminated once the oil level reached the OEM specified minimum. This way, a total mileage of approx. 20,000 km was covered in 8 months of operation.

2.2 Conventional Oil Condition Monitoring

A comprehensive description of the oil condition in terms of degradation products, residual additive levels and elemental composition is available in [5]. As this study is focussing on the tribological properties, only selected relevant degradation parameters are presented. The discussed chemical parameters taken from [5] consist of.

- oxidation via FT-IR utilizing a Tensor 27 FT-IR spectrometer (Bruker, Ettlingen, Germany) based on an in-house method of determining the absorptions at 1720 cm^{-1} ,
- residual amounts of ZDDP related to the initial amounts in the fresh oil (set to 100%) also determined by FT-IR according to an in-house method (the height of the absorption peak of the highest intensity above a local baseline laid in the spectra in the range from 1020 to 920 cm^{-1} was determined and compared to the fresh oil),
- soot loading also determined by FT-IR according to ASTM E2412 [56] based on the absorbance at 2000 cm^{-1} ,
- neutralization number (NN) according to DIN 51558 [57] by colour-indicator titration and total base number (TBN) according to DIN ISO 3771 [58] by potentiometric titration with perchloric acid utilizing a Basic Titrino 794 titrator (Metrohm AG, Herisau, Switzerland) and
- elemental composition by optical emission spectroscopy equipped with inductively coupled plasma (ICP-OES) (iCAP 7400 ICP-OES Duo, ThermoFisher, Waltham, Massachusetts, USA) after microwave treatment with nitric acid.

The reported FT-IR results are averaged from 32 transmission scans, NN and TBN from 2 titrations and elemental composition from 3 repetitions at 3 independent emission wavelengths. The applied quality assurance criterion for all

presented conventional results is a standard deviation of less than 10% of the average value.

2.3 Advanced Oil Analysis

High-resolution mass spectrometry (MS) was applied to characterize the ZDDP degradation products during the field test. Similar to conventional oil analysis, the analysis was performed according to the method described in detail in [5] and [55] and is briefly summarized below.

The oil samples were dissolved in a methanol-chloroform mixture (volumetric ratio 3:7) with a dilution factor of 1:1000. The obtained solutions were subsequently introduced into a LTQ Orbitrap XL hybrid tandem high-resolution mass spectrometer (ThermoFisher, Waltham, Massachusetts, USA), applying direct infusion with a flow rate of $5\text{ }\mu\text{L}/\text{min}$.

As ionization method, electrospray ionization (ESI) was selected. Measurements were performed in negative ion mode. As sheath gas nitrogen, as cooling and collision gas helium were applied, performing low-energy collision-induced dissociation (CID). The parent ions and the generated product ions were detected by the orbitrap detector at a resolution of 60,000 (at full width at half maximum, FWHM). The mass over charge measurements were all acquired with an accuracy of at least 5 ppm.

Data processing and interpretation were performed with the software Xcalibur version 2.0.7 and Mass Frontier version 6.0 (ThermoFisher, Waltham, Massachusetts, USA).

2.4 Tribological Analysis of the Engine Oil Samples

Friction and wear properties of 6 selected used oil samples were measured via an SRV® 5 model tribometer (Optimol Instruments Prüftechnik, Munich, Germany) according to the methodology presented in [8]. Table 2 shows an overview of the contact configuration and the experimental parameters.

The test specimens were polished before the experiments to adjust the average surface roughness to approx. $0.1\text{ }\mu\text{m}$, hence, ensuring a defined and uniform surface for all measurements. Furthermore, the SRV® tests were conducted under controlled environmental conditions, where the ambient temperature ($24.9\text{--}28.6\text{ }^\circ\text{C}$) and relative humidity ($30.6\text{--}38.6\%$) were continuously monitored.

The coefficient of friction (CoF) was determined by the SRV® instrument continuously during the 120 min test duration. Wear volume on both the SRV® ball and disc was determined by confocal 3D microscopy according to [59] and [60]. In doing so, the sample surface was cleaned in a 0.05 M disodium ethylenediaminetetraacetate (EDTA) solution at room temperature for 2 min to remove all adsorbed chemical species. The 3D topography data of

Table 2 Configuration and operating conditions of the tribometrical experiments

Parameters of the tribocontact			
Contact	Ball on disc	Ball dimension (mm)	10
Mode	Oscillation	Disc dimensions (mm)	10×7.9
Material (ball and disc)	100Cr6	Hardness (ball and disc)	HRc 62
Experimental parameters			
Oil quantity (mL)	~0.1	Temperature (°C)	100
Load (N)	50	Stroke (mm)	1
Frequency (Hz)	30	Duration (min)	120
Mean contact pressure (GPa)	1.2	Maximal contact pressure (GPa)	1.7

the sample were measured by a Leica DCM8 microscope (Leica Microsystems, Wetzlar, Germany) with an approx. 150 nm lateral and 2 nm vertical resolution. The reported wear volume is calculated based on the comparison to a reference surface before the tribometrical experiment.

The reported values of CoF and wear volume are averaged from two identical experiments per oil sample, if not indicated otherwise.

2.5 Determination of the Tribofilm Composition via XPS

The chemical information of the tribofilm was collected by using the X-ray photoelectron spectroscopy (XPS) with Thermo Scientific™ Theta Probe Angle-Resolved X-ray Photoelectron Spectrometer (ARXPS), according to the method described in detail in [55]. The instrument was equipped with a monochromatic Al K α X-ray source and a hemispherical analyser (ThermoFisher, Waltham, Massachusetts, USA). XPS analysis was performed prior to the wear measurements, immediately after the completion of the SRV® experiment, on both the ball as well as the disc, to ensure no alteration of the tribofilm on the sample surface.

The base pressure used in analytical chamber was around 3×10^{-10} mbar (UHV conditions), employing monochromatic Al K α radiation ($h\nu = 1486,6$ eV) to acquire core-level XPS spectra from the samples. The high-resolution spectra were acquired at 50 eV pass energy, 0.1 eV step size and 100 μ m spot resolution (single spot). Measurements are reported after removal of < 1 nm (10 s sputtering) of the sample surface via Ar $^{+}$ (3 kV, 1 μ A) ion bombardment to remove potential contaminations. The spectra were processed with the Avantage Data System software supplied with the XPS instrument using Gaussian–Lorentzian peak fitting. Only a single survey scan was performed per SRV® specimen.

The depth profiles of the tribofilms resulting from the fresh and final used oil were also investigated. In doing so, a repetition SRV® test was performed using the two oil samples, identically to the conditions presented in 2.4 (please note that no wear measurement was performed in

this case). Accordingly, the depth profiles also deliver some information regarding the repeatability of the processes and analytical measurements. Depth profiles of the SRV® discs were investigated under the same conditions as the overall composition (surveys), over the sputtering area of 1×1 mm, through Ar $^{+}$ (3 kV, 1 μ A) ion bombardment. For depth profiles, the conversion factor from sputter current to depth was set to 0.2 nm/(s mm 2 μ A). Depth profiling on the SRV® balls was not performed, due to the sample geometry.

3 Results and Discussion

3.1 Summary of the Chemical Parameters

Table 3 summarizes the chemical parameters of the tested engine oil samples. A detailed description of the parameters as well as an interpretation is presented in [5]. During the field test, oil samples oxidize and accumulate organic acids (oxidation products), which results in a NN increase. As the base reserve neutralizes the originated organic acids, a decrease of the TBN is visible.

The ZDDP antiwear additive is used up in the tribocontact as well as during thermo-oxidative degradation processes, consequently depletes. Soot originates in the engine as an oxidation by-product, accordingly, it accumulates during the field test.

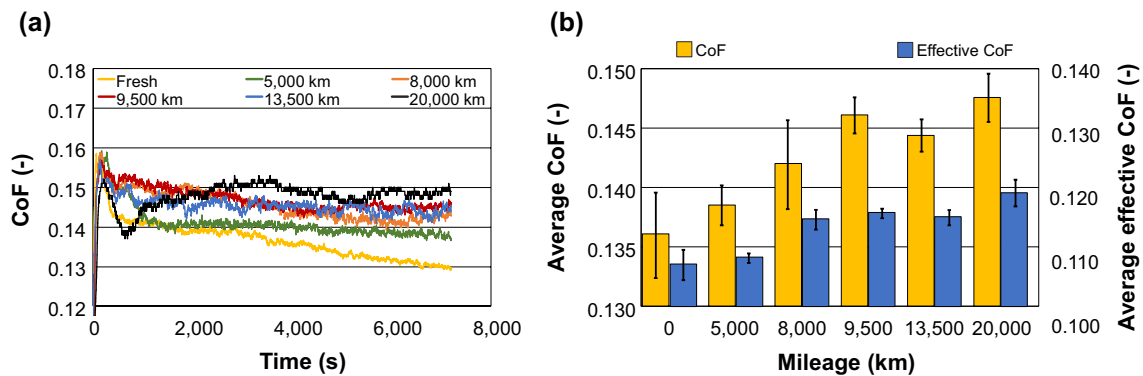
Regarding the elemental composition, the accumulation of iron (Fe) from engine wear is visible. The typical additive elements, calcium (Ca), phosphorus (P) sulphur (S) and Zinc (Zn) show only minor changes, some accumulation of Ca and Zn is visible due to the loss of volatile base oil components [7, 8], as well as some decrease in the sulphur content due to formation of volatile sulphur containing compounds [8], but the overall differences to the fresh oil are marginal.

3.2 Friction Properties

Figure 1a displays the propagation of the CoF during the SRV® experiments (only one determination per oil sample is displayed). As shown, the CoF of the fresh oil is the

Table 3 Chemical parameters of the engine oil samples

Mileage (km)	0	5000	8000	9500	13,500	20,000
Oxidation (A/cm)	0.0	7.5	10.6	12.3	19.1	30.2
NN (mgKOH/g)	1.6	1.7	2.6	2.8	4.5	5.6
TBN (mgKOH/g)	6.5	6.0	5.1	4.8	3.7	3.1
ZDDP (%)	100.0	46.1	32.2	8.8	6.8	6.5
Soot loading (A/cm)	0.0	2.5	3.3	4.3	4.4	5.3
Fe content (ppm)	5	11	19	24	37	66
Ca content (ppm)	1900	2150	2000	2050	2050	2100
P content (ppm)	720	760	730	770	810	720
S content (ppm)	2350	2150	2050	2050	2000	2250
Zn content (ppm)	880	910	880	930	990	960

**Fig. 1** a: CoF curve of the SRV® experiments b Average CoF and average effective of the engine oils

lowest among the samples and shows a decreasing trend from approx. 3000 s onwards, which indicates the effect of the present friction modifier additives. The used oil samples show an overall increasing CoF level with the mileage, and the decreasing trend of the CoF curve is not as pronounced as in case of the fresh oil sample. These effects indicate the degradation of the friction modifier additives, but further investigations with mass spectrometry methods are needed to uncover the exact structures and degradation mechanisms responsible. Furthermore, in case of the samples with the mileage of 13,500 and 20,000 km, respectively, some instability, fluctuation of the CoF is visible. This phenomenon can most probably be attributed to the higher soot loading and general (wear) particle content which might result in the formation and subsequent breakdown of agglomerates in the engine oil, hence, in the momentarily decrease and increase in friction values. Moreover, Dörr et al. observed less stable friction in case of artificially altered lubricants, which can be attributed to the degradation of ZDDP and the formation of less stable tribofilms [55]. In principle, it can be assumed that both processes occur simultaneously and therefore contribute to the higher variations in friction to some degree.

Figure 1b shows the average CoF and the average effective CoF of the oil samples, averaged from both experiments,

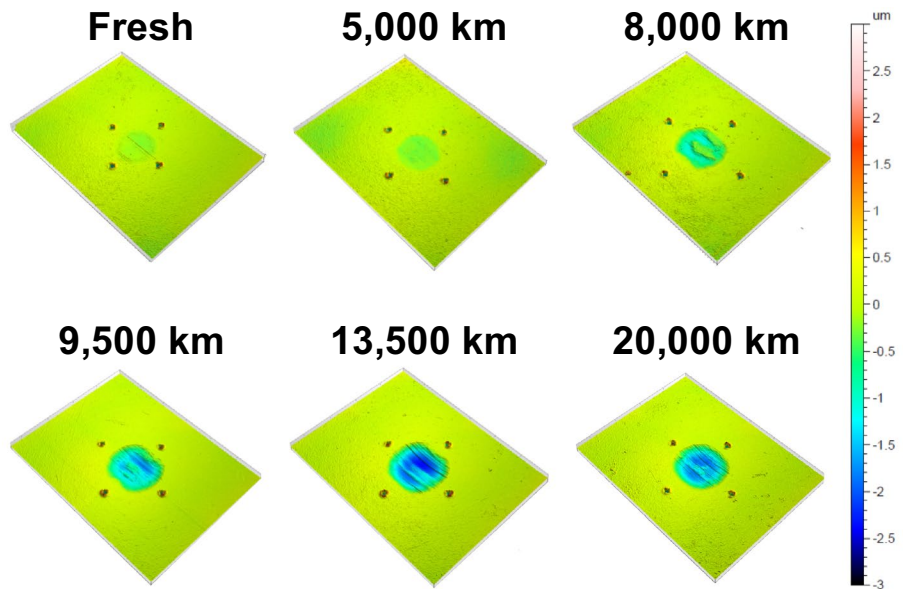
excluding the run-in phase (first 1800 s). CoF is calculated from the maximal force during each stroke, while effective CoF is based on the average force during the individual strokes. Accordingly, effective CoF is more indicative of the increase in friction losses during engine operation (fuel economy).

The averaged values once again clearly show, how the friction is increasing during the utilization of the engine oil. The differences of the CoF between the 9,500 km, 13,500 km and 20,000 km samples are considered insignificant. The total increase in friction is significant and is close to 9% in CoF and over 10% in effective CoF during the oil change interval, which has negative effects on the fuel economy of the vehicle. This highlights the importance of considering oil condition during the operation of vehicles to ensure optimal economical parameters. It has to be noted that the effective CoF values show a significantly lower standard deviation (± 1 standard deviation shown) and, accordingly, are more sensitive to show differences between the oil samples.

3.3 Wear Properties

Figure 2 displays the 3D topography images of the SRV® balls after the removal of the tribofilm. The steady increase

Fig. 2 Wear volume images of the wear scars of SRV® test balls



in the wear scar area as well as the wear volume is shown, which indicates the deterioration of the wear properties of the engine oil during its service life.

Figure 3a displays the measured wear volumes on discs and on balls of both SRV® experiments with the respective engine oil samples. As shown, the applied tribological approach displays a proper reproducibility (Please note that the respective error bars of the wear volume data are presented on Fig. 12 only). The wear on the SRV® balls increases significantly with the mileage, whereas wear on the SRV® discs shows a slight decrease after 5000 km, followed by a steady increase. Dörr et al. obtained similar results when investigating artificially altered lubricants. They also demonstrated a slight decrease in wear in the beginning of the artificial alteration process [55], which was attributed to the availability of ZDDP degradation products, which were acting more reactive compared to the original ZDDP

additive. This is comparable to the presented results and shows, that the initial phase of ZDDP degradation is likely resulting in a decrease in wear, due to the ‘activation’ of the antiwear additive. This decrease in wear was only detectable on the SRV® disc to a significant extent in case of the presented used oils. Differences between the balls and discs are expected, as the ball is under a steady state condition during the SRV® experiments, whereas parameters on the disc change continuously, as the ball reciprocates during the individual strokes. Barnes et al. also outlined in a review on ZDDP degradation, that both an increase and a decrease in wear is possible, depending on the respective degradation mechanism [61]. It is conceivable, that the degradation products in the oil present after 5,000 km mileage have a positive effect on the tribofilm formation under non-steady-state conditions, which results in a brief reduction of the wear rate on the SRV® disc only.

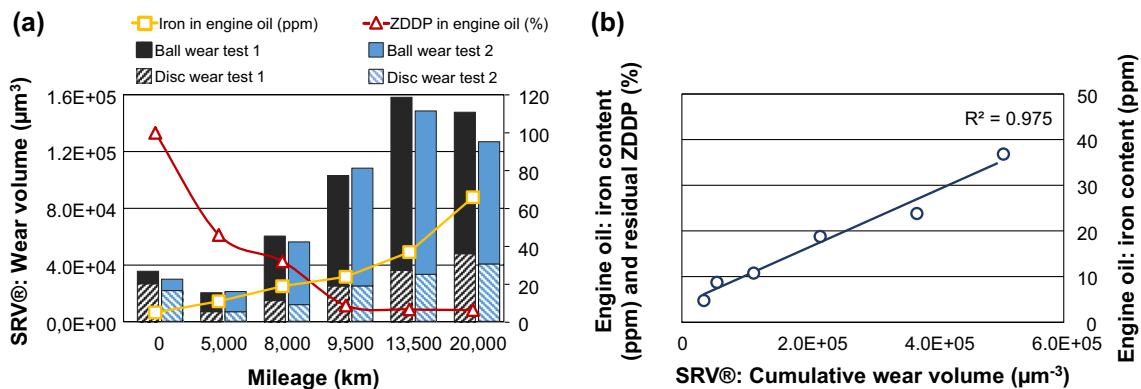


Fig. 3 a Measured wear volume of the SRV® balls and discs, correlated with the residual ZDDP content and the iron content of the engine oil b Iron content of the engine oil (engine wear) over cumulative SRV® wear volume

The authors previously reported on differences in the wear mechanism in petrol and diesel vehicles, based on a fleet study utilizing a large number of passenger cars [3]. Petrol vehicles displayed an increase in engine wear mainly due to ZDDP depletion and the subsequent loss of wear protection, whereas abrasive wear due to high soot loading was characteristic for diesel vehicles [3]. Accordingly, since the investigated vehicle is fuelled by petrol, it is assumed that the impact of ZDDP degradation is deterministic on wear and investigated in detail. Nevertheless, soot loading and the resulting abrasive effects definitely have significant impact on the wear properties, but the available data do not allow the determination of the extent.

Figure 3a also displays the residual ZDDP content determined by FT-IR of the engine oil samples. It is visible, that the wear rate significantly increases after 5000 km mileage, where the ZDDP is largely depleted. The total wear volume (sum of the ball and disc wear, as shown by the stacked columns) increases until 13,500 km mileage steadily and seems to level out afterwards, as the 20,000 km sample shows comparable total wear volume to the 13,500 km sample, similarly to the CoF. In fact, the overall increase in wear volume is close to 420% during the lifetime of the engine oil. This highlights the key importance of the wear protection additives in the reliable operation of lubricated systems. (Please note that the mechanism of ZDDP degradation is discussed in detail in 3.4 and 3.5).

Furthermore, the iron content of the engine oil (indicative of the engine wear) is also displayed in Fig. 3a. The increase in engine wear and the increase in wear during the model tribometer experiments are following similar trends, suggesting good comparability of the wear mechanisms. The iron content of the engine oil (engine wear) and the measured wear volume in the model tribometer experiments is once again displayed in Fig. 3b. Since the iron particles resulting

from engine wear are accumulating during operation, the cumulative wear volume from the SRV® tests is presented, to ensure comparability. As displayed, the relationship of the two parameters is largely linear ($R^2=0.975$), which indicates that the laboratory wear test method is adequate and correlates correctly with behaviour of the engine oil samples.

3.4 Tribofilm Composition via XPS

The analysed tribofilms mainly consist of carbon (C), oxygen (O), Ca, P, S and Zn.

Figure 4a displays the measured carbon content in the respective tribofilms and Fig. 4b shows the corresponding depth profile on the SRV® disc of the fresh (0 km) and final used oil samples (20,000 km). Carbon, together with oxygen, is one of the main components of the tribofilms, accounting for approx. 20–35 at. % in total. In detail, carbon content of the tribofilms is mainly aliphatic hydrocarbons, but oxidized species, e.g. ethers and aldehydes as well as carbonates were also identified as minor components. The observable variation in the carbon concentration is attributed to experimental XPS measurements uncertainties, furthermore, no clear trend can be observed during the lifetime of the engine oil. Carbon is mainly observable on a thin layer on the sample surface, concentration diminishes rapidly with sputtering depth. The final used oil displays a slightly higher carbon content in the tribofilm compared to the fresh oil in the depth profile, but the overall differences are minor and are not considered significant.

Figure 5a displays the measured oxygen content in the tribofilms and the NN of the respective engine oil samples. Figure 5b shows the XPS oxygen depth profile on the SRV® tested disc of the fresh and final used oil samples. Oxygen, besides carbon, is one of the main components of the tribofilm, accounting for approx. 45–55 at. %.

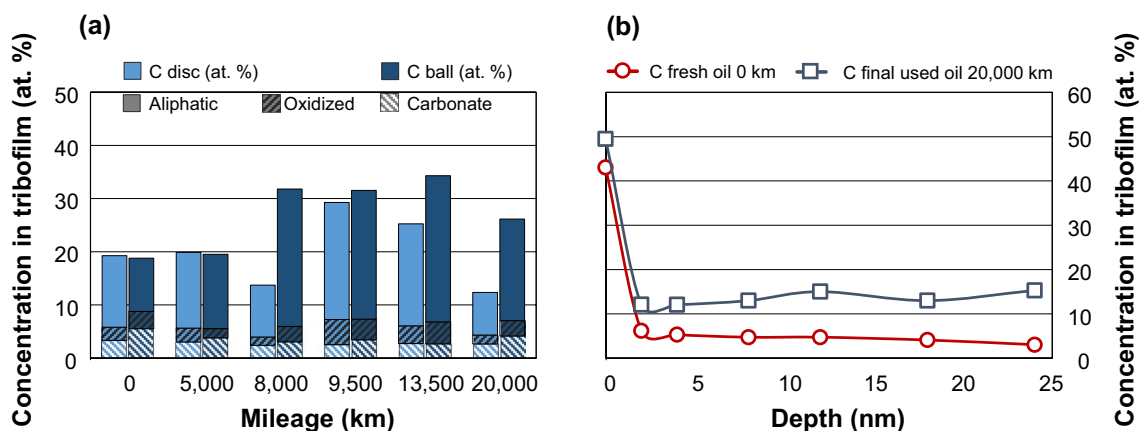


Fig. 4 a XPS Carbon content of the respective tribofilms b XPS Carbon depth profile on the SRV® tested discs of the fresh and final used oil samples

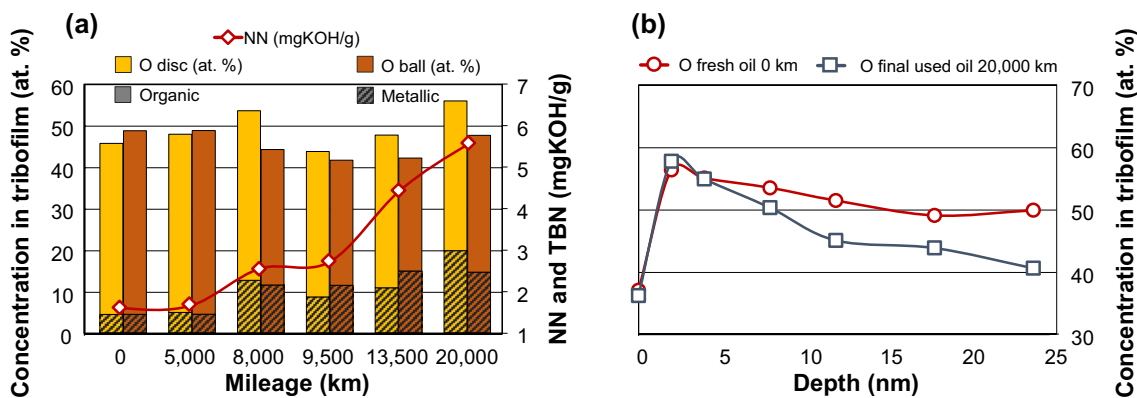


Fig. 5 a: XPS Oxygen content of the tribofilms and the NN of the respective oil samples **b** XPS Oxygen depth profile on the SRV® tested discs of the fresh and final used oil samples

is predominately present as organic compounds, but some metallic bounded oxygen (metal oxides) is also visible. The samples show a comparable oxygen concentration in the tribofilms, although the relative ratio of the metal oxides seems to increase at higher oil mileages. This correlates with the increasing NN and might be attributed to (tribo)corrosive effects. The medial distribution of oxygen shows a maximum approx. 2 nm below the surface and a decreasing trend afterwards. The fresh and final used oils display comparable trends regarding oxygen distribution.

Figure 6a shows the measured calcium content in the tribofilms and the NN as well as the TBN of the respective oil samples. Additionally, the calcium content of the engine oil samples is also displayed. Calcium accounts for approx. 8–16 at. % of the observed tribofilms and is present as carbonate, oxide and sulphate. The calcium content of the tribofilms is decreasing during the lifetime of the engine oil and shows a good correlation with the NN increase and the TBN decrease. This effect is especially prevalent on

the SRV® ball but also visible on the disc to some degree, and previous studies also showed a similar decrease in the calcium content of the tribofilm during artificial ageing of engine oils [55]. During the depletion of the base reserve, the calcium carbonate base reserve additive neutralizes the organic acids which are originating from the oxidation of the oil samples [3, 5]. The base reserve consists of calcium carbonate (salt) particles suspended in detergent micelles in the fresh oil [3, 62]. The neutralization reactions are resulting in water, carbon dioxide and ‘free’, hydrated calcium ions [3]. It is possible that the state of calcium, whether it is present in a salt or as ‘free’ ions, has an influence on the tribofilm formation process. It seems likely that calcium carbonate particles representing the original state of Ca in engine oils are incorporated with a higher probability in the tribofilm. This might be linked to chemically induced corrosive effects (‘acidic attacks’) on the surface, but further investigations are needed to accurately describe the responsible physicochemical processes. The final used oil displays a TBN of

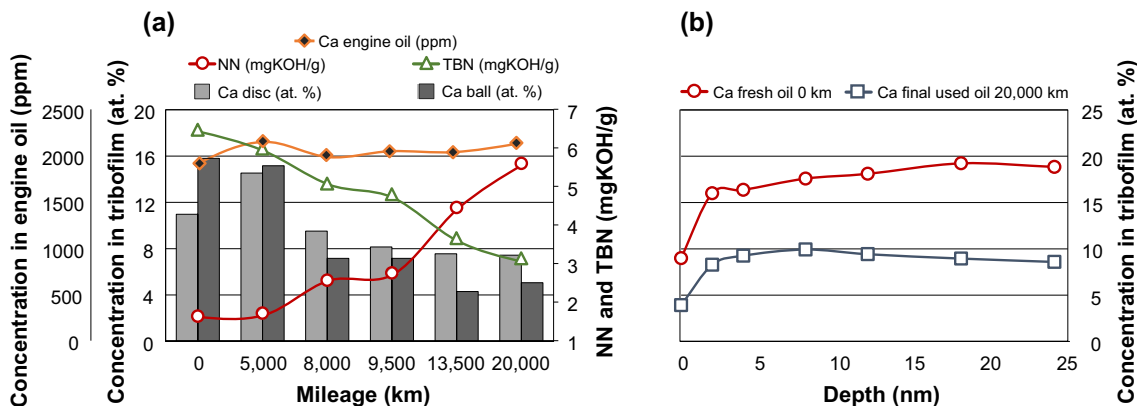


Fig. 6 a: XPS Calcium content of the tribofilms and NN as well as TBN of the respective oil samples **b**: XPS Calcium depth profile on the SRV® tested discs of the fresh and final used oil samples

approx. 3 mgKOH/g, which is attributed to difficulties with the applied method, as the titration with strong perchloric acid detects other basic substances than the base reserve as well, e.g. dispersant bases, even diphenylamine antioxidants and ashless amine additives [55, 63]. Accordingly, the base reserve is considered to be depleted at this point.

Additionally, the calcium content of the engine oil samples stays close to constant during the lifetime of the engine oil, which clearly indicates that the changes in the tribofilm composition are linked to chemical changes of the additives, not to the depletion of calcium from the engine oil.

Figure 6b shows the depth profile of calcium on the SRV® disc of the fresh and final used oil samples. The calcium concentration is somewhat lower directly on the surface but close to constant from 2 to 24 nm depth. The final used oil sample displays significantly less calcium in the tribofilm compared to the fresh oil.

The following section addresses the changes in tribofilm formation correlated with the degradation of the present ZDDP antiwear additive. ZDDP tribofilms are mainly consisting of glassy Fe/Zn polyphosphate on top of a thin iron sulphide / zinc sulphide base layer. The tribofilm is usually deposited in ‘pads’, accordingly, shows an inhomogeneous lateral structure [52]. Figure 7 shows a schematic representation of a typical ZDDP tribofilm (figure produced from data reported in [52]).

Figure 8a displays the determined phosphorus content in the tribofilms, the residual amount of ZDDP and the

phosphorus content of the engine oil samples. The analysed tribofilms are consisting of approx. 4–10 at. % phosphorus present as phosphates. The phosphorus concentration decreases in the tribofilms during the oil change interval, which correlates well with the ZDDP depletion. This result is expected, as the depletion of the ZDDP results in the loss of wear protection, the loss of the ability of the engine oil to form a glassy Fe/Zn polyphosphate film on the surface [52]. Similar to the calcium concentration, the phosphorus concentration shows no significant change in the engine oil samples, accordingly, the differences in the tribofilm composition can once again be attributed to additive degradation, changes in the organic structures and not the depletion of zinc from the engine oil. Dörr et al. also found a decrease in the calcium content of the tribofilm by artificially aged lubricants [55]. Figure 8b shows the XPS depth profile of phosphorus on the SRV® disc of the fresh and final used oil samples. The medial distribution of phosphorus is relatively uniform under the uppermost surface layer, but the tribofilm resulting from the fresh engine oil displays significantly higher phosphorus content compared to the tribofilm formed by the final used oil sample.

Figure 9a shows the measured zinc content in the tribofilms as well as in the engine oil samples and the residual amount of ZDDP in the respective oils. The analysed tribofilms are consisting of approx. 1–3 at. % zinc, present as oxides and sulphides. One exception is the SRV® disc of the fresh oil, where a significantly higher concentration

Fig. 7 Schematic representation of a typical ZDDP tribofilm (based on the data reported in [52])

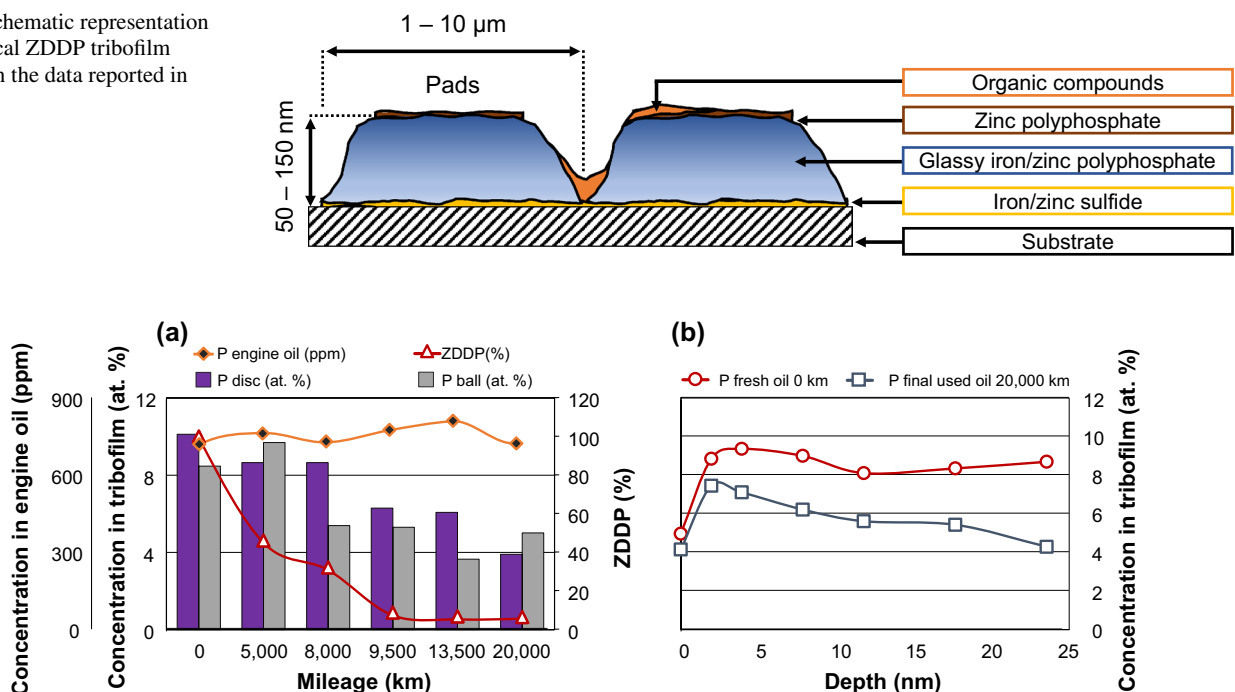


Fig. 8 a XPS Phosphorus content of the tribofilms and residual ZDDP in the respective oil samples b depth profile on the SRV® tested discs of the fresh and final used oil samples

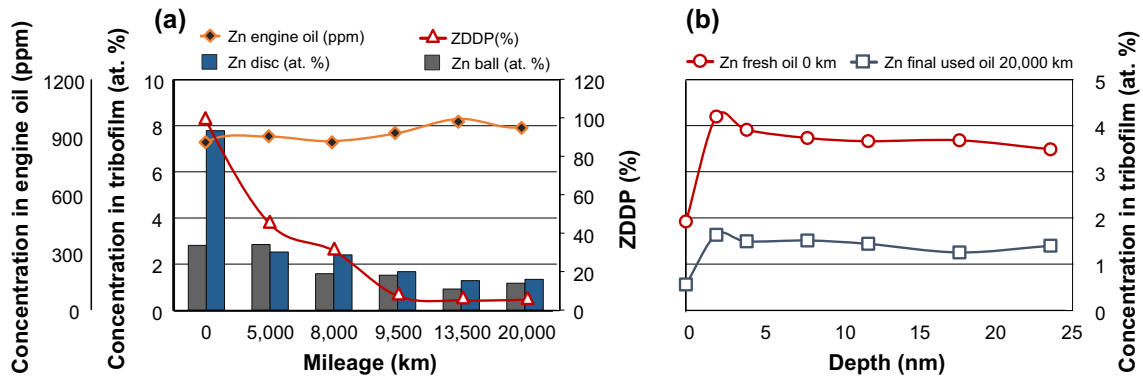


Fig. 9 a XPS Zinc content of the respective tribofilms and residual ZDDP in the oil samples b depth profile on the SRV® tested discs of the fresh and final used oil samples

was measured. This might be attributed to the already mentioned differences in the state and temperature of the ball and disc, or simply to a local inhomogeneity at the site of the respective survey measurement. The zinc concentration in the tribofilm, similar to phosphorus shows a decreasing trend during the lifetime of the engine oil, which is also consistent of the depletion of ZDDP and the loss of surface protection (glassy Fe/Zn polyphosphate film). Meanwhile, the engine oil samples are displaying a close to constant zinc concentration, which once again highlights that degradation of the additive structures is responsible for the changes in the tribofilm composition. The results of Dörr *et al.* are also confirming a decrease in the zinc content of the tribofilm during the artificial alteration of engine oils [55]. Regarding depth profiles, the zinc distribution is also relatively consistent beneath the surface layer, as displayed in Fig. 9b. The fresh engine oil once again forms a tribofilm different from the final used oil, namely the zinc concentration is significantly higher as in the final used oil sample. Crobu *et al.* reported in [40] that the polyphosphate chain length is dependent on the

zinc concentration in the tribofilm. Accordingly, it is likely that the fresh and used oils formed films with significantly different polyphosphate chain length in this case as well. It is conceivable that this difference is linked to the deteriorating wear properties as well.

Figure 10a displays the sulphur content in the tribofilms and the engine oil samples, as well as the residual amount of ZDDP in the oil samples. The sulphur content in the tribofilms is generally low (approx. 2–4 at. %). This is consistent with the structure of a typically formed ZDDP tribofilm, where sulphides are only present as minor components in the base layer [52]. The sulphur is mainly present as sulphide and sulphate, with some minor amount of sulphite in some samples. It has to be noted, that the sulphur content of the tribofilm formed by the fresh engine oil contains only sulphides, most likely as iron and zinc sulphide (both ZDDP-film components), while films formed by the used oils contain similar amounts of sulphides and sulphates in most cases. Dörr *et al.* also obtained similar results in case of laboratory aged engine oils, namely that the relative amount of sulphates increases with engine oil degradation, while the

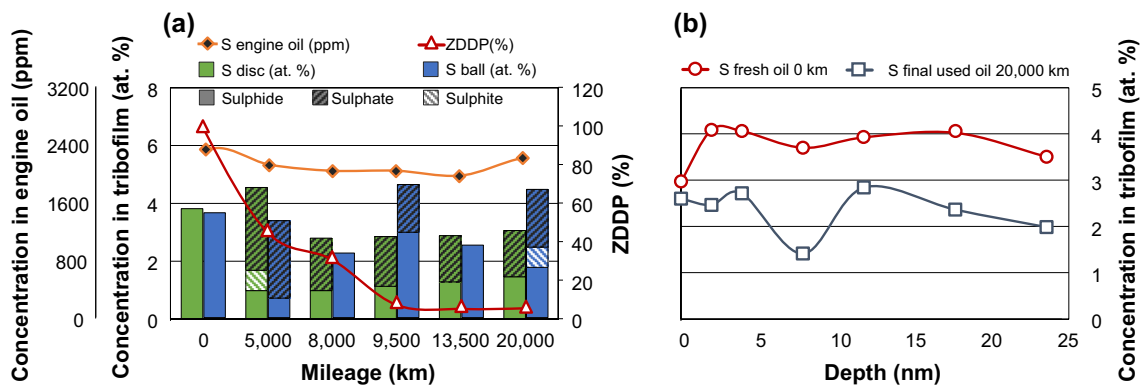


Fig. 10 a XPS Sulphur content of the tribofilms and residual ZDDP in the respective oil samples b XPS Sulphur depth profile on the SRV® tested discs of the fresh and final used oil samples

overall sulphur content remains relatively unaffected [55]. This can be attributed to tribocorrosive effects between the degradation products, namely acids and the substrate surface [55], which is only pronounced in case of degraded lubricants. Somayaji *et. al* reported that a higher sulphate concentration in the tribofilms generally results in poorer wear protection [64], which is consistent with the obtained results. Figure 10b shows the depth profile of sulphur which is relatively unaffected in the tribofilms formed by both the fresh and used engine oils. The fresh engine oil results in a tribofilm with a slightly higher sulphur concentration, but the overall differences are quite small and should be interpreted accordingly.

Figure 11a shows the iron concentration in the tribofilms and residual ZDDP content of the engine oils. Iron accounts for approx. 2–14 at. % of the formed tribofilms and is mainly as iron oxide and as iron sulphide present. Some low amount of metallic iron and iron disulphide can also be detected, mainly in case of the oil samples with higher mileage. The iron content shows a very significant increase after the almost complete degradation of the ZDDP anti-wear additive. This is consistent with the observed increase in wear. Similarly, the final used oil sample forms a tribofilm that contains significantly more iron on all observed depths. Iron concentration in the tribofilm correlates with the surface coverage by the ZDDP tribofilm. Due to the paddy structure of such films, some of the (iron) substrate is not covered, accordingly, visible for the XPS although the sputtering depth (24 nm) is significantly lower than the average film thickness (50–150 nm). It is assumed that the increase in the iron concentration is mainly caused by the decrease in ZDDP film coverage, i.e. approx. 4% of the surface was not covered in case of the fresh oil, which increased to over 12% during the lifetime of the engine oil.

3.5 Correlation of the ZDDP Degradation and the Tribofilm Formation

High-resolution MS was applied to generate further, in-depth knowledge about the degradation products of ZDDP, since commonly available FT-IR based methods, as presented in 3.4, are affected by interference of degradation products of ZDDP [5] and do not give any insights on the additive degradation on the molecular level, only a sum parameter.

The degradation mechanism of the present ZDDP additive was discussed extensively in [5] and [55]. The investigation with high-resolution MS revealed, that dihexyl dithiophosphate (m/z 297.111) is the main component of ZDDP in this specific engine oil formulation. The dihexyl dithiophosphate decomposes rapidly during the formation of organic degradation products, namely dihexyl thiophosphate (m/z 281.134; one sulphur atom replaced with oxygen) and dihexyl phosphate (m/z 265.156; both sulphur atoms replaced with oxygen). Afterwards, the elimination of alkyl side chains [55] and the origination of sulphuric acid (m/z 96.960) and phosphoric acid (m/z 96.970) are observable [5, 55].

The original dihexyl dithiophosphate could not be detected by MS after 6000 km mileage. At the same time, dihexyl thiophosphate increased swiftly to the peak intensity that was detected after 2,000 km. Afterwards, the dihexyl thiophosphate depleted rapidly until approx. 6000 km and was detected only at negligible amounts until the end of the field test. Dihexyl phosphate was observed from the beginning of the field test and was detectable in high amounts after the depletion of both dihexyl dithiophosphate and dihexyl thiophosphate. Dihexyl phosphate also showed fluctuating intensities, which did not allow to derive an exact trend, nevertheless it remained at high levels until the end of the service life of the engine oil. The origination of sulphuric and phosphoric acid was observable after approx. 9000 km

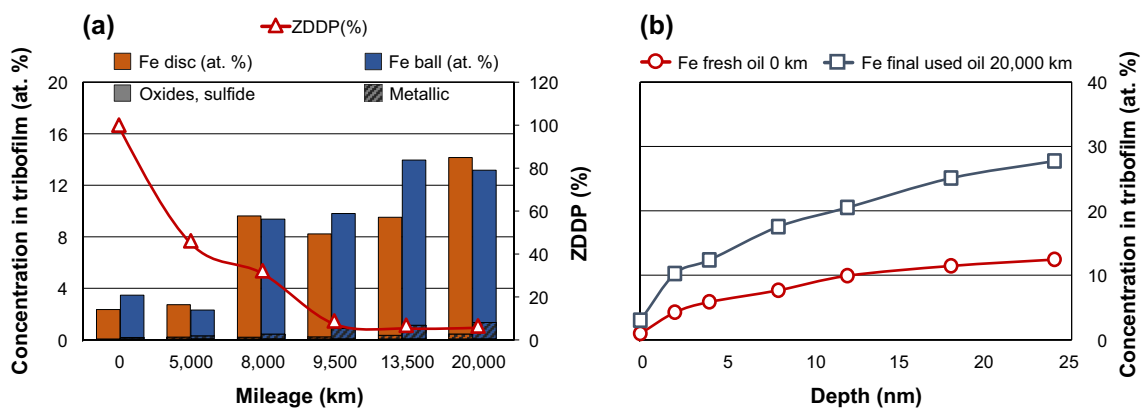


Fig. 11 **a** XPS Iron content of the tribofilms and residual ZDDP in the respective oil samples **b** XPS Iron depth profile on the SRV® tested discs of the fresh and final used oil samples

mileage, where both inorganic acids, although fluctuating in intensity, remained present until the end of the field test in a higher concentration.

As the degradation of ZDDP was very rapid, concentrating to the first approx. 6000 km of the field test, the whole dataset is presented again, as already published in [5], to achieve a reasonable time-resolution. Figure 12a (top) shows the determined composition of the tribofilm on the SRV® ball regarding ZDDP-relevant elements, namely iron, phosphorus and zinc. Figure 12b (middle) displays the propagation of the intensity of dihexyl dithiophosphate and its degradation products, dihexyl thiophosphate, dihexyl phosphate, sulphuric acid and phosphoric acid throughout the entire field test. The detected total ion current (TIC) is presented in arbitrary units. Figure 12c (bottom) shows the associated average total wear volume (sum of the wear volume measured on the ball and the disc, averaged from the two

SRV® experiments) and average CoF (averaged from 1800 to 7200 s) of the oil samples.

It is visible, that the phosphorus and zinc concentration decreases, the iron concentration increases significantly right after dihexyl dithiophosphate (original additive) and dihexyl thiophosphate (first degradation product) are both depleted. This occurred around 6000 km total mileage. The remaining dihexyl phosphate (final degradation product) performs sub-par regarding wear protection compared to the dihexyl dithiophosphate and dihexyl thiophosphate, indicated by the ‘sharp’ change in tribofilm composition, which also corresponds to the significant increase in wear (close to 420% at the end of the field test compared to the fresh oil). Furthermore, the deterioration of the friction properties indicated by the increasing average CoF is also visible. Overall, 3 ‘phases’ can be observed (as denoted by dotted lines in Fig. 12):

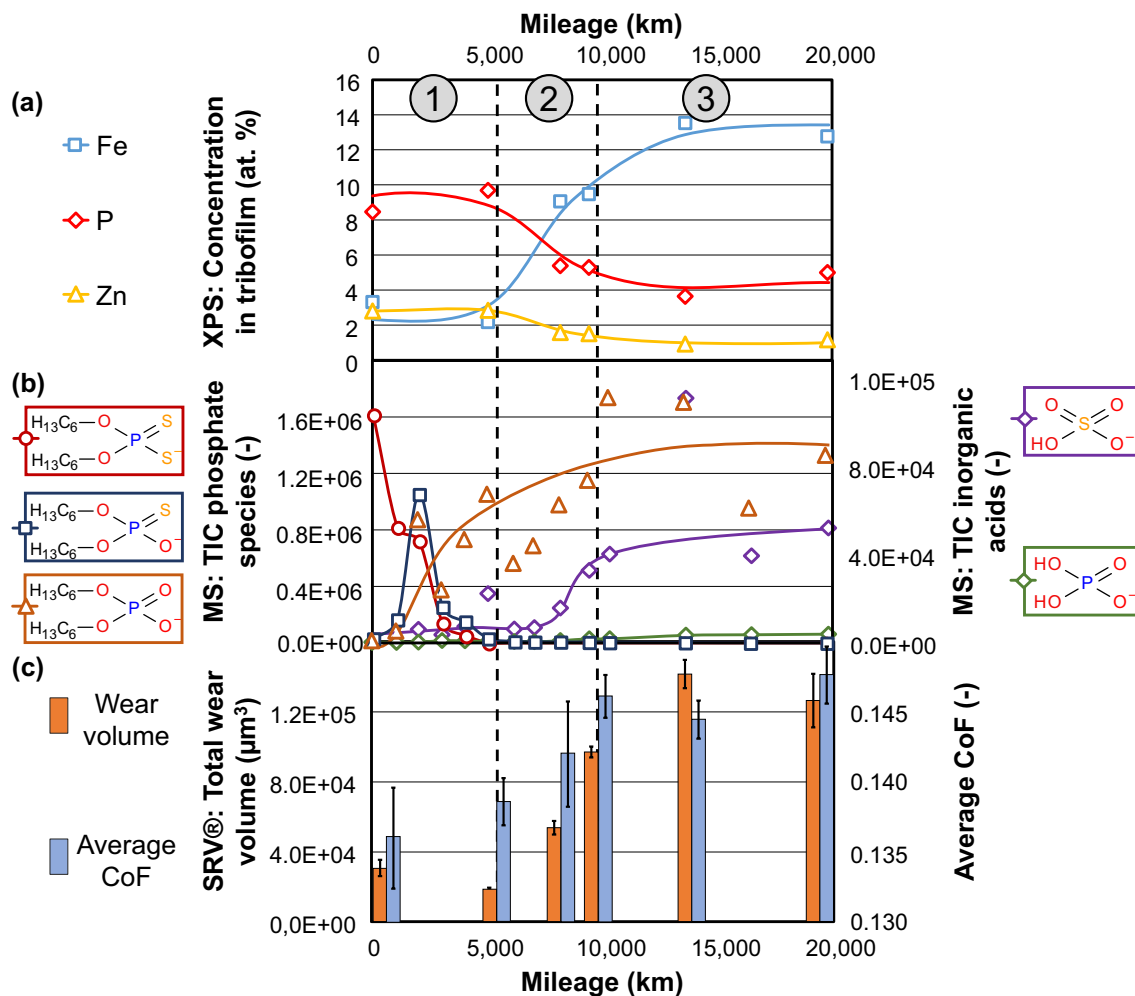


Fig. 12 a Comparison of the tribofilm composition, **b** the ESI MS intensity of dihexyl dithiophosphate and its respective degradation products, dihexyl thiophosphate, dihexyl phosphate, sulphuric acid

and phosphoric acid **c**): the respective average total wear volume and average CoF (± 1 standard deviation is shown as error bars) The displayed lines only facilitate better visualization

- 1: Induction phase, which is characterized by the depletion of the original dihexyl dithiophosphate and the originated dihexyl phosphate. The tribofilm composition is unaffected until the complete depletion of both structures, and the wear volume shows a slight decrease, due to the ‘activation’ [55] of the antiwear additives by partial degradation of the original ZDDP and the origination of organic ZDDP degradation species, e.g. dialkyl thiophosphates.
- 2: Transient phase, which is characterized by the origination of dihexyl phosphate and later sulphuric (and phosphoric) acid. The tribofilm composition changes rapidly, and a decrease in the phosphorus and zinc concentration and an increase in iron concentration (decrease in surface coverage) are observable. The wear volume increases significantly.
- 3: Degraded steady state phase, where the additive degradation and the resulting tribofilm composition reaches a new steady state. The wear volume is significantly higher than in the induction or transient phases, possibly due to tribocorrosive effect of the now present sulphuric and phosphoric acid but shows no further increase. The 2 final samples with 13,500 and 20,000 km mileage, respectively, are showing very similar tribofilm composition and well-comparable friction and wear performance as well.

It is conceivable, that dihexyl phosphate would also deplete at an even higher mileage, which once again might result in a sharp change in tribofilm composition and a further increase in wear, as it was the case in [55], but the investigation of this effect has lower technical relevance, as it would occur way over 20,000 km vehicle mileage, which exceeds common (long life) oil change intervals. Please note, that the deterioration of the friction properties cannot be attributed to the depletion of ZDDP only, but to a complex interplay of physiochemical deterioration, such as friction modifier degradation as well as soot and particle accumulation.

4 Conclusions

The tribological performance of an engine oil during a typical oil change interval of 20,000 km was observed. The collected oil samples showed deteriorating friction and wear, where the friction increased with close to 9% and wear with close to 420% during the service life of the engine oil. The observed wear in the SRV® model tribometer and the iron accumulation in the engine oil (engine wear) showed a good linear correlation, which indicates that the relatively simple tribometrical approach indicates changes in an in-service ICE correctly.

Determination of the tribofilm composition of the model test showed that calcium, phosphorus and zinc concentration decreased, while iron concentration increased during the service life of the engine oil. The decreases can be correlated to additive depletion; in case of calcium, the depletion of the base reserve, and in case of phosphorus, zinc and iron, the depletion of ZDDP and the subsequent increase in wear are responsible for the changes in the tribofilm composition. In case of sulphur, a decrease in sulphides and an increase in sulphates were observed with the propagation of engine oil degradation, which hints the presence of tribocorrosive effects.

Comparison of the tribofilm composition with high-resolution mass spectrometry data on ZDDP and its respective degradation products of the engine oil showed that the tribofilm composition changes right after the depletion of dialkyl dithiophosphates and dialkyl thiophosphates. First, a ‘transition phase’ occurs while the dihexyl phosphate and sulphuric and phosphoric acid originate, then a new ‘steady state’ is reached. The remaining dialkyl phosphates are producing a tribofilm with lower phosphorus and zinc and higher iron concentration. Correlation with the wear results suggests that this film composition is sub-par with regard to wear protection and that tribocorrosive effects might be present to a greater extent.

It is noteworthy, how well real used oil samples and artificially altered lubricants correlate in both the additive degradation on the molecular level and the resulting tribofilm composition. The results presented by Dörr et al. in [55] showed a very well-comparable ZDDP degradation pathway, although further propagated in laboratory alterations. The resulting changes were also similar; a decrease in zinc and phosphorus and an increase in sulphates were observed with advancing engine oil degradation, which is well comparable to the presented results. This highlights that although field tests are necessary to validate laboratory-based methods, a carefully selected artificial alteration can replace them in numerous cases, which results in a considerable reduction in development cost and time.

Acknowledgements Presented results were realized in research projects with financial support from the participating project partners and the Austrian COMET program (Project InTribology, No. 872176). The COMET program is funded by the Austrian Federal Government and concerning InTribology by the provinces of Lower Austria and Vorarlberg. The authors would like to thank all researchers of AC2T research GmbH who were involved in the study and in particular Thomas Wopelka for providing the vehicle and driving thousands of kilometres reliably and safely in the name of science, among others.

Author Contributions Conceptualization: AA, CB, MF and ND. Data curation and visualization: AA. Formal analysis, investigation, validation and methodology: AA, JB and SB. Funding acquisition: MF and ND. Project administration: CB. Resources: AA, CB, JB, SB, MF and ND. Software: not applicable. Supervision: ND. Writing—original draft: AA, CB, JB. Writing—review and editing: CB, MF.

Funding Austrian COMET program (Project InTribology, No. 872176).

Data Availability All data and materials comply with field standards.

Code Availability Not applicable.

Declarations

Conflict of interest All Authors declare that they have no competing interest.

References

1. ACEA: Fuel types of new passenger cars in the EU. ACEA figures (2021). <https://www.acea.auto/figure/fuel-types-of-new-passenger-cars-in-eu/>. Accessed 19 July 2021
2. Schwarze, H., Brouwer, L., Knoll, G., Schlerege, F., Müller-Frank, U., Kopnarski, M., Emrich, S.: Ölalterung und Verschleiß im Ottomotor (engl.: oil ageing and wear in the petrol engine). *Motortechnische Zeitschrift (MTZ)* **69**, 878–886 (2008)
3. Agocs, A., Nagy, A.L., Tabakov, Z.S., Perger, J., Rohde-Brandenburger, J., Schandl, M., Besser, C., Dörr, N.: Comprehensive assessment of oil degradation patterns in petrol and diesel engines observed in a field test with passenger cars—conventional oil analysis and fuel dilution. *Tribol. Int.* (2021). <https://doi.org/10.1016/j.triboint.2021.107079>
4. Agocs, A., Budnyk, S., Frauscher, M., Ronai, B., Besser, C., Dörr, N.: Comparing oil condition in diesel and gasoline engines. *Ind. Lubr. and Tribol.* (2020). <https://doi.org/10.1108/ILT-10-2019-0457>
5. Dörr, N., Agocs, A., Besser, C., Ristic, A., Frauscher, M.: Engine oils in the field: a comprehensive chemical assessment of engine oil degradation in a passenger car. *Tribol. Lett.* (2019). <https://doi.org/10.1007/s11249-019-1182-7>
6. Repka, M., Dörr, N., Brenner, J., Gabler, C., McAleese, C., Ishigo, O., Koshima, M.: Lubricant-surface interactions of polymer coated engine bearings. *Tribol. Int.* (2017). <https://doi.org/10.1016/j.triboint.2017.01.017>
7. Besser, C., Agocs, A., Ronai, B., Ristic, A., Repka, M., Jankes, E., McAleese, C., Dörr, N.: Generation of engine oils with defined degree of degradation by means of a large scale artificial alteration method. *Tribol. Int.* (2019). <https://doi.org/10.1016/j.triboint.2018.12.003>
8. Agocs, A., Budnyk, S., Besser, C., Ristic, A., Frauscher, M., Ronai, B., Dörr, N.: Production of used engine oils with defined degree of degradation in a large-scale device: correlation of artificially altered oils with field samples. *ACTA Technica Jaurinensis* (2020). <https://doi.org/10.14513/actatechjaur.v13.n2.546>
9. Mourhatch, R., Aswath, P.B.: Tribological behavior and nature of tribofilms generated from fluorinated ZDDP in comparison to ZDDP under extreme pressure conditions—Part I: structure and chemistry of tribofilms. *Tribol. Int.* (2011). <https://doi.org/10.1016/j.triboint.2010.10.018>
10. Mourhatch, R., Aswath, P.B.: Tribological behavior and nature of tribofilms generated from fluorinated ZDDP in comparison to ZDDP under extreme pressure conditions—Part II: morphology and nanoscale properties of tribofilms. *Tribol. Int.* (2011). <https://doi.org/10.1016/j.triboint.2010.10.035>
11. Rastogi, R.B., Maurya, J.L., Jaiswal, V.: Low sulfur, phosphorus and metal free antiwear additives: synergistic action of salicylaldehyde *N*(4)-phenylthiosemicarbazones and its different derivatives with Vanlube 289 additive. *Wear* (2013). <https://doi.org/10.1016/j.wear.2012.10.003>
12. Kim, B.H., Jiang, J.C., Aswath, P.B.: Mechanism of wear at extreme load and boundary conditions with ashless anti-wear additives: analysis of wear surfaces and wear debris. *Wear* (2011). <https://doi.org/10.1016/j.wear.2010.10.058>
13. Najman, M.N., Kasrai, M., Bancroft, G.M.: Chemistry of antiwear films from ashless thiophosphate oil additives. *Tribol. Lett.* (2004). <https://doi.org/10.1023/B:TRIL.0000032448.77085.f4>
14. Qu, J., Luo, H., Chi, M., Ma, C., Blau, P.J., Dai, S., Viola, M.B.: Comparison of an oil-miscible ionic liquid and ZDDP as a lubricant anti-wear additive. *Tribol. Int.* (2014). <https://doi.org/10.1016/j.triboint.2013.11.010>
15. Zhou, Y., Qu, J.: Ionic liquids as lubricant additives: a review. *ACS Appl. Mater. Interfaces* (2017). <https://doi.org/10.1021/acsami.6b12489>
16. Pejaković, V., Kronberger, M., Kalin, M.: Influence of temperature on tribological behaviour of ionic liquids as lubricants and lubricant additives. *Lubr. Sci.* (2013). <https://doi.org/10.1002/lis.1233>
17. Pejaković, V., Tomastik, C., Dörr, N., Kalin, M.: Influence of concentration and anion alkyl chain length on tribological properties of imidazolium sulfate ionic liquids as additives to glycerol in steel-steel contact lubrication. *Tribol. Int.* (2016). <https://doi.org/10.1016/j.triboint.2016.01.034>
18. Kronberger, M., Pejaković, V., Gabler, C., Kalin, M.: How anion and cation species influence the tribology of a green lubricant based on ionic liquids. *Proc. Inst. Mech. Eng. Part J* (2012). <https://doi.org/10.1177/21350650112459012>
19. Sharma, V., Dörr, N., Erdemir, A., Aswath, P.B.: Interaction of phosphonium ionic liquids with borate esters at tribological interfaces. *RSC Adv.* (2016). <https://doi.org/10.1039/C6RA11822D>
20. Sharma, V., Dörr, N., Erdemir, A., Aswath, P.B.: Antiwear properties of binary ashless blend of phosphonium ionic liquids and borate esters in partially formulated oil (No Zn). *Tribol. Lett.* (2019). <https://doi.org/10.1007/s11249-019-1152-0>
21. Xue, Q., Liu, W.: Tribochemistry and the development of AW and EP oil additives—a review. *Lubr. Sci.* (1994). <https://doi.org/10.1002/lis.3010070107>
22. Spikes, H.: The history and mechanisms of ZDDP. *Tribol. Lett.* (2004). <https://doi.org/10.1023/B:TRIL.0000044495.26882.b5>
23. Nicholls, M.A., Do, T., Norton, P.R., Kasrai, M., Bancroft, G.M.: Review of the lubrication of metallic surfaces by zinc dialkyl-dithiophosphates. *Tribol. Int.* (2005). <https://doi.org/10.1016/j.triboint.2004.05.009>
24. Palacios, J.M.: Thickness and chemical composition of films formed by antimony dithiocarbamate and zinc dithiophosphate. *Tribol. Int.* (1986). [https://doi.org/10.1016/0301-679X\(86\)90093-9](https://doi.org/10.1016/0301-679X(86)90093-9)
25. Suominen Fuller, M.L., Rodriguez Fernandez, L., Massoumi, G.R., Lennard, W.N., Kasrai, M., Bancroft, G.M.: The use of X-ray absorption spectroscopy for monitoring the thickness of antiwear films from ZDDP. *Tribol. Lett.* (2000). <https://doi.org/10.1023/A:1019195404055>
26. Taylor, L., Dratva, A., Spikes, H.A.: Friction and wear behavior of zinc dialkyl-dithiophosphate additive. *Tribol. Trans.* (2000). <https://doi.org/10.1080/10402000008982366>
27. Fujita, H., Spikes, H.A.: The formation of zinc dithiophosphate antiwear films. *Proc. Inst. Mech. Eng. Part J* (2004). <https://doi.org/10.1243/21350650041762677>
28. Varlot, K., Kasrai, M., Martin, J.M., Vacher, B., Bancroft, M.G., Yamaguchi, E.S., Ryason, P.R.: Antiwear film formation of neutral and basic ZDDP: influence of the reaction temperature and of the concentration. *Tribol. Lett.* (2000). <https://doi.org/10.1023/A:1019162529554>

29. Zhang, J., Spikes, H.: On the mechanism of ZDDP antiwear film formation. *Tribol. Lett.* (2016). <https://doi.org/10.1007/s11249-016-0706-7>
30. Fujita, H., Spikes, H.A.: Study of zinc dialkyldithiophosphate antiwear film formation and removal processes. Part II: kinetic model. *Tribol. Trans.* (2005). <https://doi.org/10.1080/05698190500385187>
31. Barros Bouchet, M.I., Martin, J.M., Le-Mogne, T., Vacher, B.: Boundary lubrication mechanisms of carbon coatings by MoDTC and ZDDP additives. *Tribol. Int.* (2005). <https://doi.org/10.1016/j.triboint.2004.08.009>
32. Morina, A., Neville, A.: Understanding the composition and low friction tribofilm formation/removal in boundary lubrication. *Tribol. Int.* (2007). <https://doi.org/10.1016/j.triboint.2007.02.001>
33. Morina, A., Neville, A.: Tribofilms: aspects of formation, stability and removal. *J. Phys. D: Appl. Phys.* **40**, 5476–5487 (2007). <https://doi.org/10.1088/0022-3727/40/18/S08>
34. Ghanbarzadeh, A., Piras, E., Nedelcu, I., Brizmer, V., Wilson, M.C.T., Morina, A., Dowson, D., Neville, A.: Zinc dialkyl dithiophosphate antiwear tribofilm and its effect on the topography evolution of surfaces: a numerical and experimental study. *Wear* (2016). <https://doi.org/10.1016/j.wear.2016.06.004>
35. Morina, A., Green, J., Neville, A., Priest, M.: Surface and tribological characteristics of tribofilms formed in the boundary lubrication regime with application to internal combustion engines. *Tribol. Lett.* (2003). <https://doi.org/10.1023/B:TRIL.0000003065.37526.84>
36. Parsaeian, P., Ghanbarzadeh, A., Van Eijk, M.C.P., Nedelcu, I., Neville, A., Morina, A.: A new insight into the interfacial mechanisms of the tribofilm formed by zinc dialkyl dithiophosphate. *Appl. Surf. Sci.* (2017). <https://doi.org/10.1016/j.apsusc.2017.01.178>
37. Neville, A., Morina, A., Haque, T., Woong, M.: Compatibility between tribological surfaces and lubricant additives—how friction and wear reduction can be controlled by surface/lube synergies. *Tribol. Int.* (2007). <https://doi.org/10.1016/j.triboint.2007.01.019>
38. Berbezier, I., Martin, J.M.: The adverse effect of carbon in mild wear with ZDDP lubricant additive. *Tribol. Int.* (1988). [https://doi.org/10.1016/0301-679X\(88\)90080-1](https://doi.org/10.1016/0301-679X(88)90080-1)
39. Heuberger, R., Rossi, A., Spencer, N.D.: Pressure dependence of ZnDTP tribochemical film formation: a combinatorial approach. *Tribol. Lett.* (2007). <https://doi.org/10.1007/s11249-007-9267-0>
40. Crobu, M., Rossi, A., Mangolini, F., Spencer, N.D.: Chain-length-identification strategy in zinc polyphosphate glasses by means of XPS and ToF-SIMS. *Anal. Bioanal. Chem.* (2012). <https://doi.org/10.1007/s00216-012-5836-7>
41. Barros Bouchet, M.I., Righi, M.C., Philippon, D., Mambingo-Doumbe, S., Le-Mogne, T., Martin, J.M., Bouffet, A.: Tribochemistry of phosphorus additives: experiments and first-principles calculations. *RSC Adv.* (2015). <https://doi.org/10.1039/C5RA00721F>
42. Kim, B.H., Mourhatch, R., Aswath, P.B.: Properties of tribofilms formed with ashless dithiophosphate and zinc dialkyl dithiophosphate under extreme pressure conditions. *Wear* (2010). <https://doi.org/10.1016/j.wear.2009.10.004>
43. Gosvami, N.N., Bares, J.A., Mangolini, F., Konicek, A.R., Yablon, D.G., Carpick, R.W.: Mechanisms of antiwear tribofilm growth revealed in situ by single-asperity sliding contacts. *Science* (2015). <https://doi.org/10.1126/science.1258788>
44. Bancroft, G., Kasrai, M., Fuller, M., Yin, Z., Tan, K.H.: Mechanisms of tribochemical film formation: stability of tribo- and thermally-generated ZDDP films. *Tribol. Lett.* (1997). <https://doi.org/10.1023/A:1019179610589>
45. Soltanahmadi, S., Morina, A., Van Eijk, M.C.P., Nedelcu, I., Neville, A.: Experimental observation of zinc dialkyl dithiophosphate (ZDDP)-induced iron sulphide formation. *Appl. Surf. Sci.* (2017). <https://doi.org/10.1016/j.apsusc.2017.04.023>
46. Dawczyk, J., Ware, E., Ardakani, M., Russo, J., Spikes, H.: Use of FIB to study ZDDP Tribofilms. *Tribol. Lett.* (2018). <https://doi.org/10.1007/s11249-018-1114-y>
47. Minfray, C., Martin, J.M., Esnouf, C., Le Mogne, T., Kersting, R., Hagenhoff, B.: A multi-technique approach of tribofilm characterisation. *Thin Solid Films* (2004). [https://doi.org/10.1016/S0040-6090\(03\)01064-2](https://doi.org/10.1016/S0040-6090(03)01064-2)
48. Piras, F.M., Rossi, A., Spencer, N.D.: Growth of tribological films: in situ characterization based on attenuated total reflection infrared spectroscopy. *Langmuir* (2002). <https://doi.org/10.1021/la0202733>
49. Piras, F.M., Rossi, A., Spencer, N.D.: Combined in situ (ATR FT-IR) and ex situ (XPS) Study of the ZnDTP-Iron Surface Interaction. *Tribol. Lett.* (2003). <https://doi.org/10.1023/A:1024800900716>
50. Dorgham, A., Neville, A., Ignatiyev, K., Mosselmans, Morina, A.: An in situ synchrotron XAS methodology for surface analysis under high temperature, pressure, and shear. *Rev. Sci. Instrum.* (2017). <https://doi.org/10.1063/1.4973354>
51. Dorgham, A., Parsaeian, P., Neville, A., Ignatiyev, K., Mosselmans, F., Masuko, M., Morina, A.: In situ synchrotron XAS study of the decomposition kinetics of ZDDP tribochemical interfaces. *RSC Adv.* (2018). <https://doi.org/10.1039/C8RA04753G>
52. Johnson, D.W., Hils, J.E.: Phosphate esters, thiophosphate esters and metal thiophosphates as lubricant additives. *Lubricants* (2013). <https://doi.org/10.3390/lubricants1040132>
53. Sharma, V., Timmons, R., Erdemir, A., Aswath, P.B.: Plasma-functionalized polytetrafluoroethylene nanoparticles for improved wear in lubricated contact. *ACS Appl. Mater. Interfaces* (2017). <https://doi.org/10.1021/acsami.7b06453>
54. Sharma, V., Timmons, R.B., Erdemir, A., Aswath, P.B.: Interaction of plasma functionalized TiO₂ nanoparticles and ZDDP on friction and wear under boundary lubrication. *Appl. Surface Sci.* (2019). <https://doi.org/10.1016/j.apsusc.2019.05.359>
55. Dörr, N., Brenner, J., Ristić, A., Ronai, B., Besser, C., Pejako- vić, V., Frauscher, M.: Correlation between engine oil degradation, tribochemistry, and tribological behavior with focus on ZDDP deterioration. *Tribol Lett* (2019). <https://doi.org/10.1007/s11249-019-1176-5>
56. ASTM E2412–10. Standard practice for condition monitoring of in-service lubricants by trend analysis using fourier transform infrared (FT-IR) spectrometry. West Conshohocken: ASTM International; 2018
57. DIN 51558–1: Testing of mineral oils; determination of the neutralization number; colour-indicator titration. Deutsches Institut für Normung, Berlin, Germany (1979)
58. DIN ISO 3771: Petroleum products – Determination of base number – Perchloric acid potentiometric titration method. International Organization for Standardization, Geneva, Switzerland (2011)
59. Vorlaufer, G., Ilincic, S., Franek, F., Pauschitz, A.: Wear quantification by comparison of surface topography data. In: Wang, Q.J., Chung, Y.W. (eds.) *Encyclopedia of Tribology*, pp. 4087–4093. Springer, Boston (2013)
60. Vorlaufer, G., Prünner, D., Wopelka, T., Dörr, N.: Extracting wear information from 3D topography data. ÖTG Symposium, November 22 2018, Vienna, Austria.
61. Barnes, A.M., Bartle, K.D., Thibo, V.R.A.: A review of zinc dialkyldithiophosphates (ZDDPS): characterisation and role in the lubricating oil. *Tribol. Int.* (2001). [https://doi.org/10.1016/S0301-679X\(01\)00028-7](https://doi.org/10.1016/S0301-679X(01)00028-7)
62. Rudnick, L.R.: *Lubricant Additives—Chemistry and Applications*. Marcel Dekker Inc, New York (2003)

63. Agiral, A., Zalatan, D., Sutor, P.: Understanding total base number measurement. STLE 73th Annual Meeting & Exhibition, May 20–24 2018, Minneapolis, Minnesota, United States
64. Somayaji, A., Aswath, P.B.: The role of antioxidants on the oxidation stability of oils with F-ZDDP and ZDDP, and chemical structure of tribofilms using XANES. Tribol. Trans. (2009). <https://doi.org/10.1080/10402000902745499>
65. ÖNORM EN 228: Kraftstoffe für Kraftfahrzeuge – Unverbleite Ottokraftstoffe – Anforderungen und Prüfverfahren (engl.: Automotive fuels – Unleaded petrol - Requirements and test methods). Austrian Standards, Vienna, Austria (2016) and (2017)

Publisher's Note Springer Nature remains neutral with regard to jurisdictional claims in published maps and institutional affiliations.